

Artificial Neural Network based Maximum Powerpoint Tracking of Solar Panel

C. Anil Kumar* and N. Surekha**

Abstract : Maximum Power Point Tracking (MPPT) is necessary for Solar Photo Voltaic (SPV) system. Many algorithms such as Perturb and Observe, Incremental conductance and hill climbing are available to track the maximum power. But they have disadvantages such as high cost, difficult to implement and instable. Artificial Neural Network (ANN) is suitable for handling non-linearities, uncertainties and parameter variations in a controlled environment. The data for training neural network is determined from the simulation result of SPV array. The temperature (T) and insolation (G) are input variables to ANN and the output variable is the voltage (V) corresponding to the maximum power. This technique is implemented in the MATLAB environment.

Keywords: Maximum PowerPoint Tracking (MPPT), Artificial Neural Network (ANN), Photovoltaic Power System, Boost converter, Matlab/Simulink.

1. INTRODUCTION

Solar cell is a p-n junction fabricated in a thin wafer or layer of silicon, which converts the solar energy into electricity [1]. Photovoltaic (PV) cells have a nonlinear relationship between the current and the voltage, and the maximum power point of PV cells changes with environmental conditions such as solar irradiance and ambient temperature. Further maximum power from the photovoltaic panel is necessary to improve the efficiency.

Many techniques have been developed to provide maximum PV power. Enslin employed an integrated PV maximum-power-point tracker with soft switching to obtain the optimum efficiency [2]. Some researchers control photovoltaic characteristics to match load conditions [3]–[5]. Some systems use an online maximum power point tracking (MPPT) algorithm to obtain the maximum power point [6]–[9].

The most commonly used MPPT algorithm is Perturb & Observe (P&O) due to its simplicity. Three techniques have been proposed in the literature for implementing the P&O algorithm: reference voltage perturbation [10], [11], reference current perturbation [12], [13], and direct duty ratio perturbation [14]. The algorithm operates periodically by comparing the present value of the power output with the previous value to determine the change on the solar array voltage or current. If the magnitude of power is increasing, the perturbation will continue in the same direction in the next cycle, otherwise the perturbation direction is reversed. But this algorithm suffers from oscillations that occur around the MPP in steady state operation and also slow response speed at rapidly changing atmospheric conditions.

Hill climbing [15] operates by perturbing the system by changing the power converter duty cycle and observing its impact on the array output power. It has three major drawbacks.

(a) Slow converging to the optimum operating point.

* Assistant Professor., Department of Electrical and Electronics Engineering, Erode Builder Educational Trust's group of institutions, Erode. *E-mail:* aniljaiswalc20@gmail.com

** AssistantProfessor., Department of Electrical and Electronics Engineering, Kalaivani College of Technology, Coimbatore. *E-mail* surekha.nanda@gmail.com

- (b) At steady-state condition, the amplitude of the PV power is oscillates around the maximum point that causes system power losses.
- (c) During cloudy days when the irradiance varies quickly the operating point moves away from the maximum optimum point.

The incremental conductance method is based on the principle that the slope of the PV array curve is zero at the maximum power point [16]. This method requires high sampling rates and fast calculation of the power slope.

Artificial Neural Network is suitable for handling non-linearities, uncertainties and parameter variations in a controlled environment, which has been proposed in this thesis. The main objective of this thesis is to develop ANN based MPP tracking scheme for Solar PV system with varying environmental conditions and also to extract maximum power from the panel.

2. MODELING OF PV ARRAY

Under clean environment, Photovoltaic cells convert sunlight directly to electricity. When sunlight hits the cell, the photons are absorbed by the semiconductor atoms, freeing electrons from the negative layer. This free electron finds its path through an external circuit toward the positive layer resulting in an electric current from the positive layer to the negative layer. The equivalent circuit of the PV cell is shown in Fig. 1.

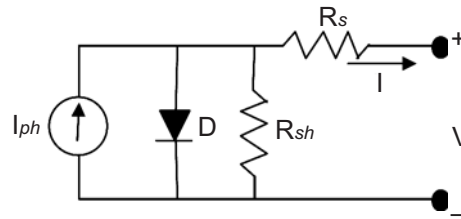


Figure 1: Equivalent circuit of PV cell

The voltage-current characteristic equation of a solar cell [18] is given as

$$I = I_{ph} - I_s \left\{ e^{\left[\frac{q(V + IR_s)}{kAT_c} \right]} \right\} - \frac{V + IR_s}{R_{sh}} \quad (1)$$

Where

- I – Solar cell current (A)
- V – Solar cell voltage (V)
- I_{ph} – Light generated current (A)
- I_s – Cell saturation current (A)
- q – Electron charge; 1.602×10^{-19} J/V
- R_s – Series resistance (ohm)
- R_{sh} – Shunt resistance (ohm)
- k – Boltzman's constant; 1.38×10^{-23} J/K
- A – Diode ideality factor
- T_c – Cell temperature (K)
- G – Insolation (W/m^2)

The light generated current or photocurrent mainly depends on the solar insolation and cell's working temperature. The intensity and spectral distribution of the solar radiation depend on the geographic position, time, day of the year, climate conditions, composition of the atmosphere, altitude, and many other factors [17]. The photocurrent is given as

$$I_{ph} = [I_{sc} + K_1 (T_c - T_{ref})]G \quad (2)$$

Where

I_{SC} – Cell’s short-circuit current at 298 K and 1 kW/m^2

T_{ref} – Reference temperature of the cell; 298K

K_1 – Short circuit temperature coefficient; $0.0017 \text{ (A/}^\circ\text{C)}$

The cell’s saturation current varies as a cubic function of the temperature and it can be expressed as

Where
$$I_s = I_{RS} \left(\frac{T_c}{T_{ref}} \right)^3 e^{\left[\frac{qE_g(T_c - T_{ref})}{T_{ref}T_c kA} \right]} \quad (3)$$

I_{RS} – Cell’s reverse saturation current at a reference temperature and solar radiation

E_g – Band-gap energy

A generalized PV model is built using Matlab/Simulink according to equation (1), (2) and (3). The model is designed and shown in Figs. 2 and 3.

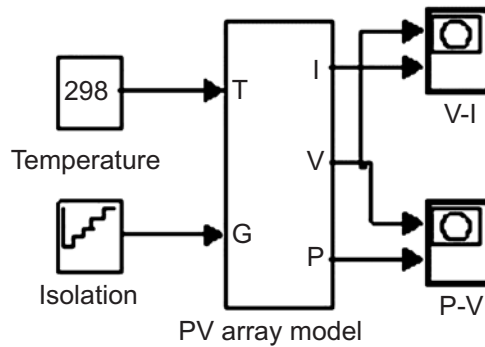


Figure 2: Masked PV model for various Insolation

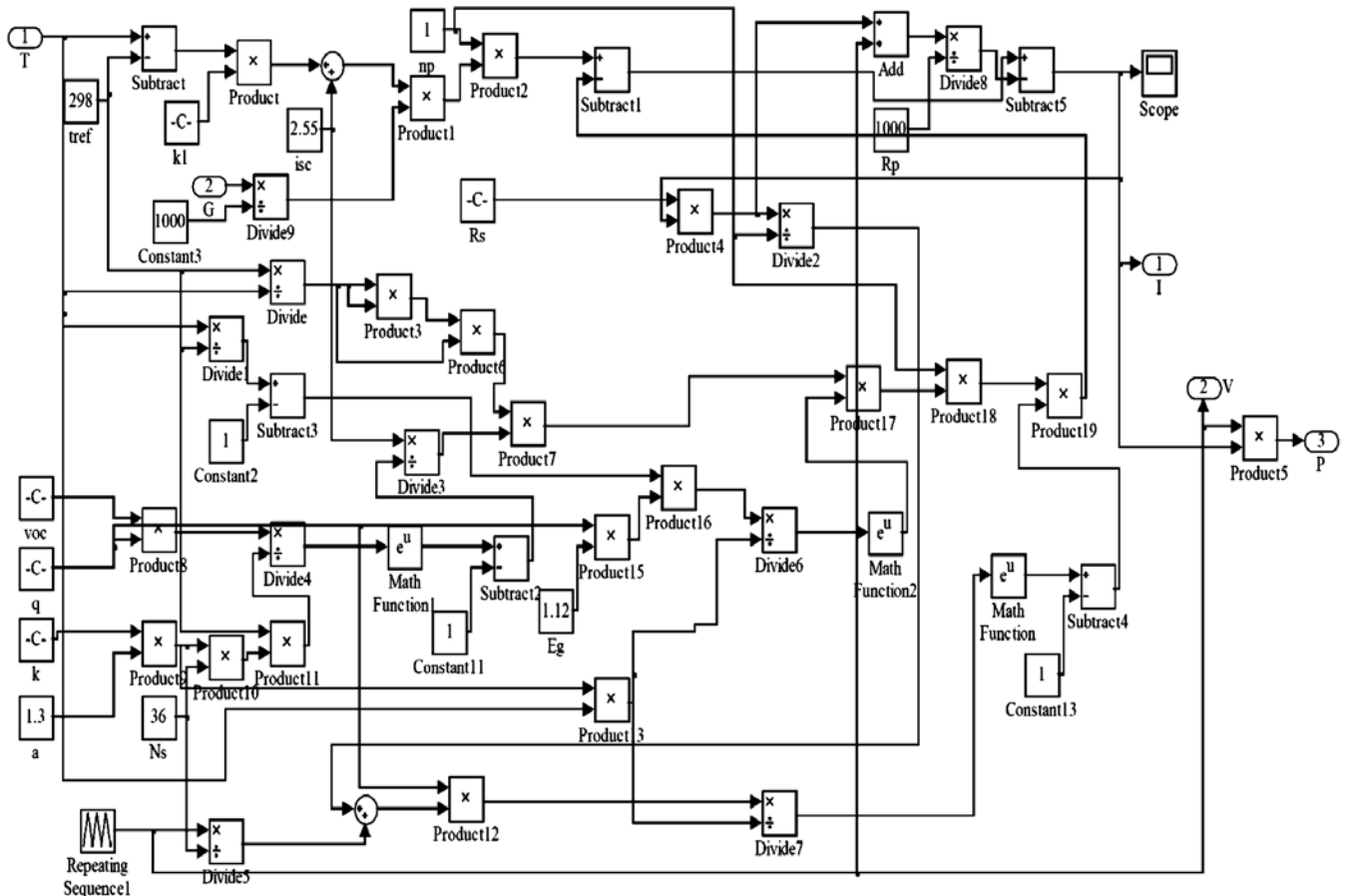


Figure 3: Simulation Diagram of PV Array model

To verify the nonlinear V-I and P-V output characteristics of the modeled PV array, the model is simulated for different insolation and temperature and is shown in Figs. 4, 5, 6 and 7.

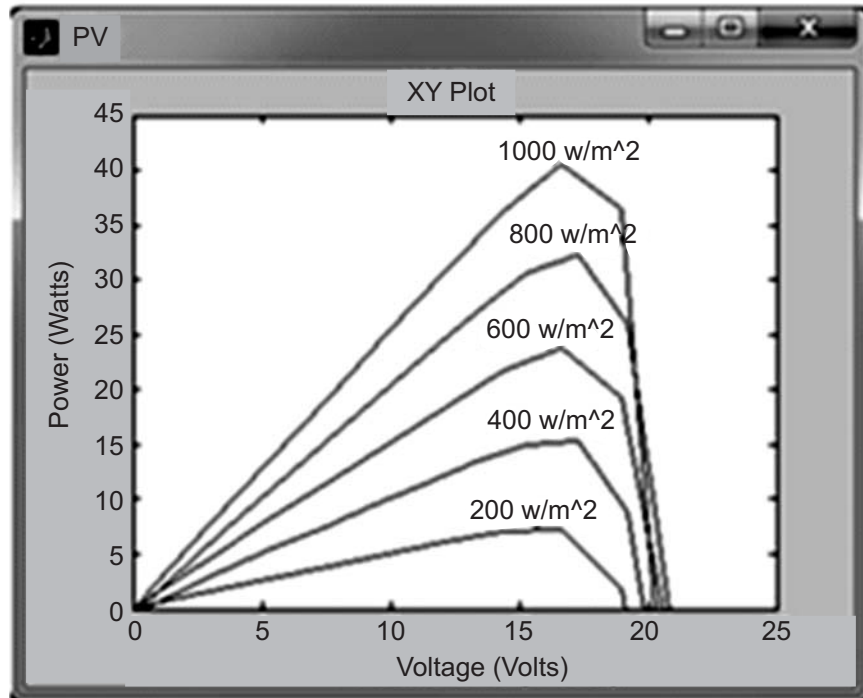


Figure 4: P-V Characteristics at different Insolation

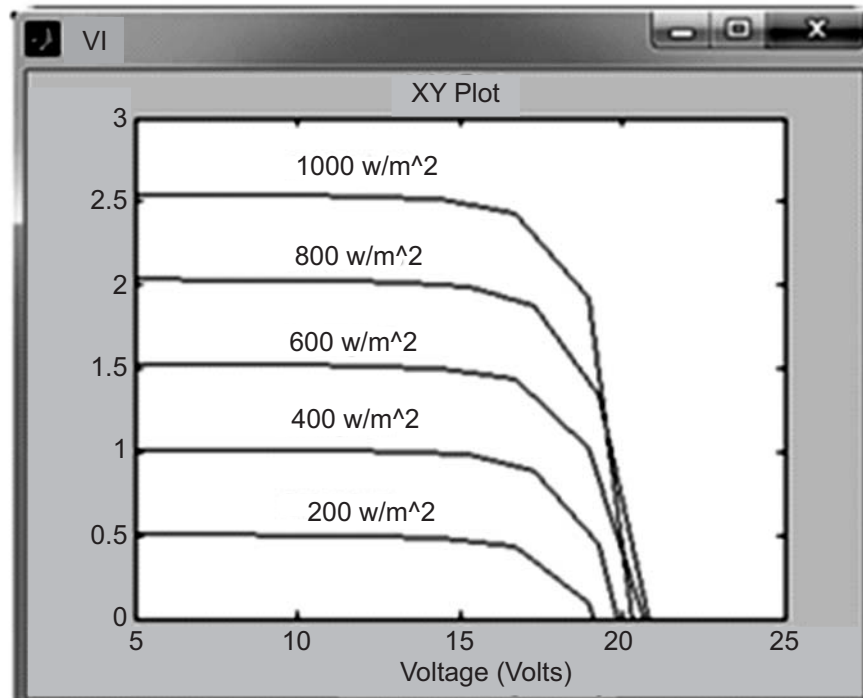


Figure 5: V-I Characteristics at different Insolation

This solar model is simulated for temperature ranging from 25°C to 75°C and for insolation from 50 W/m² to 1000 W/m² and the output voltage and current corresponding to maximum power is noted and tabulated in a worksheet. Nearly 1020 readings are taken by simulating the PV array. First 20 readings are shown in the Table 1.

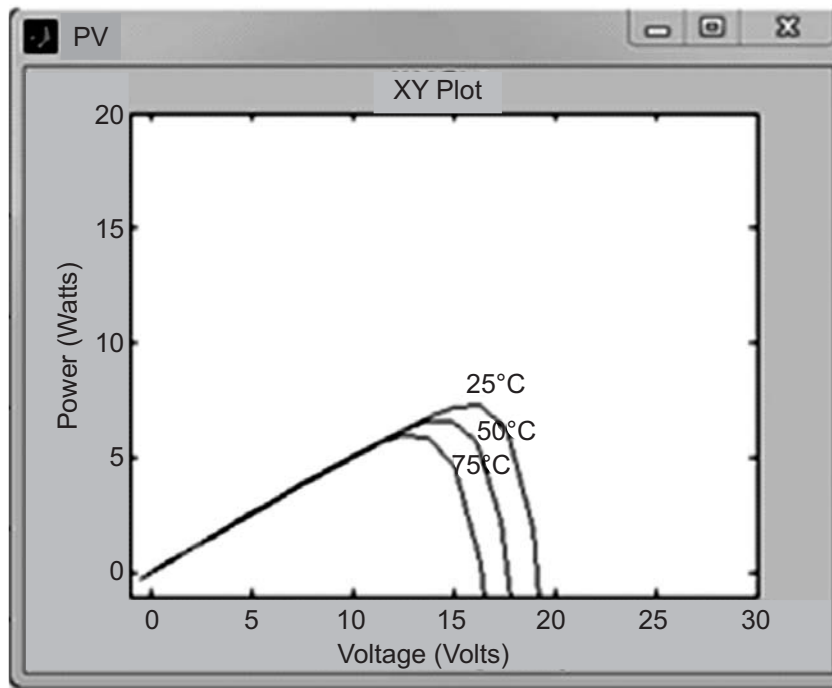


Figure 6: P-V Characteristics at different Temperature

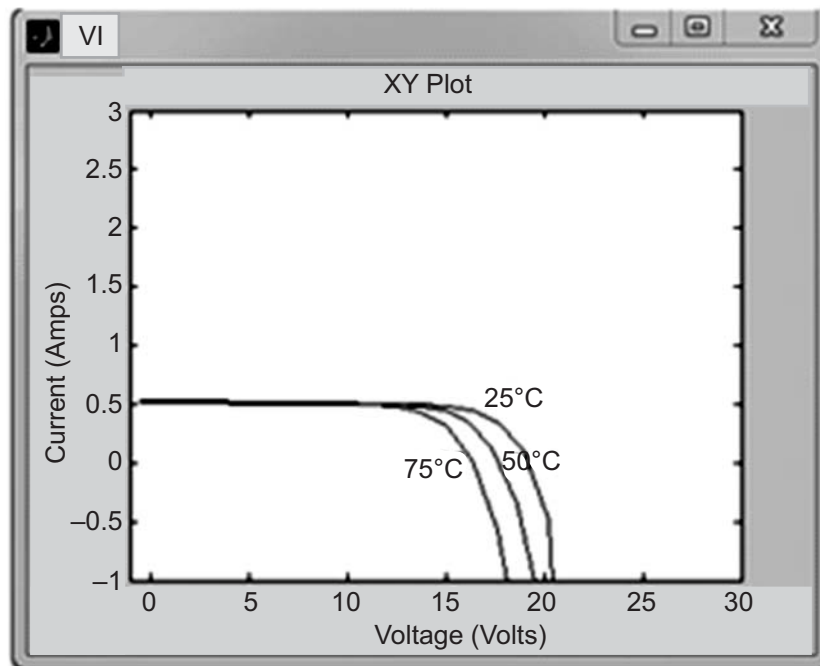


Figure 7: V-I Characteristics at different Temperature

Thus the training data for neural network is obtained. These data has to be normalized before given as input to the neural network and the output obtained will be the normalized values so they has to be converted into original values before given as input to the comparator to generate the necessary pulse. The normalized training data is given in the APPENDIX A.

3. ANN-BASED MPPT ALGORITHM

The main objective of any MPPT controller is to draw maximum power from PV modules for changing solar insolation (G) and temperature (T) conditions [19], [20]. PV module voltage is used as the control parameter and an MPPTcontroller is implemented based on the voltage (V_{MPP}) at which the PV modules

operate at the MPP. In this paper, an ANN is used to determine the reference voltage depending upon G and T. The dataset used to train the ANN is obtained using simulation results. The transfer function of the hidden layers is tangent sigmoidal and output layers is pure linear. The stopping criteria like iteration number is chosen as 1000 and goal as 0.0001. A multilayer structure including an input layer, 2 hidden layers with 8 and 10 hidden nodes are obtained based on trial-and-error method, and an output layer. The selection of the number of hidden layers is given in table 2.

Table 1
Training data for neural network

<i>Temperature(°c)</i>	<i>Insolation(w/m2)</i>	<i>Voltage (volts)</i>	<i>Current (amps)</i>	<i>Power (watts)</i>
25	50	13.51	0.1041	1.40639
	100	14.42	0.221	3.18682
	150	14.87	0.3398	5.05282
	200	15.33	0.4551	6.97668
	250	15.78	0.5655	8.92359
	300	15.78	0.6915	10.9118
	350	16.24	0.7945	12.9026
	400	16.24	0.9198	14.9375
	450	16.24	1.045	16.9708
	500	16.24	1.17	19.0008
	550	16.69	1.261	21.046
	600	16.69	1.385	23.1156
	650	16.69	1.509	25.1852
	700	16.69	1.633	27.2547
	750	16.69	1.757	29.3243
	800	16.69	1.881	31.3938
	850	16.69	2.005	33.4634
	900	17.15	2.072	35.5348
950	17.15	2.195	37.6442	
1000	17.15	2.317	39.7365	

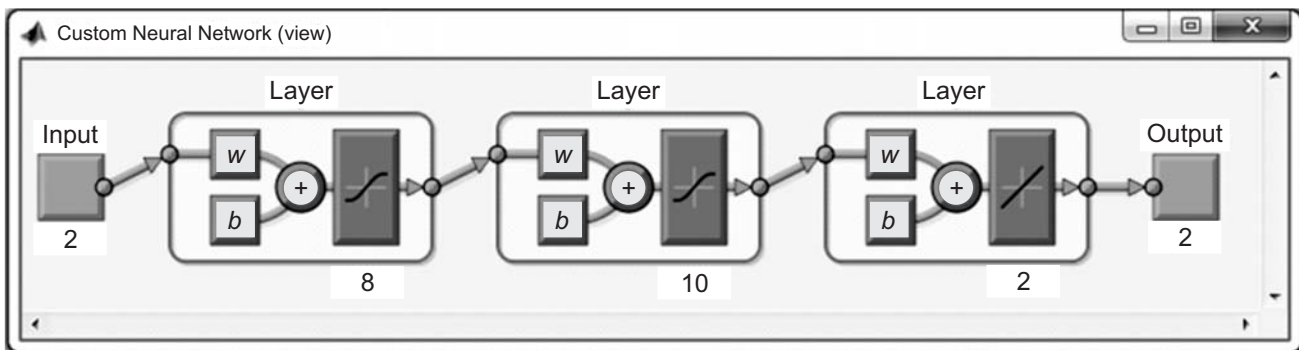


Figure 8: Feed Forward Neural Network for MPPT

Table 2
Hidden layer selection

<i>Hidden Layer 1</i>	<i>Hidden Layer 2</i>	<i>Training, R</i>	<i>EPOCHS</i>	<i>Time</i>	<i>Performance</i>
2	3	0.9987	1921	1min, 9sec	0.0001
5	5	0.9987	1089	20sec	0.0001
3	5	0.996	2000	36sec	0.000308
3	8	0.99724	2000	38sec	0.000213
8	8	0.99871	612	13sec	0.0000993
10	8	0.9987	368	8sec	0.0000999
10	10	0.99871	459	10sec	0.0000997
8	10	0.9987	402	9sec	0.0001
5	10	0.9987	1921	39sec	0.0001
2	10	0.99868	2000	38sec	0.000102
2	15	0.99508	2000	42sec	0.000379
10	15	0.9987	516	13sec	0.0001
15	20	0.99871	403	12sec	0.0000998
20	20	0.99871	449	14sec	0.0001

The trained neural network is shown in Fig. 8 and its performance plot is shown in Fig. 9.

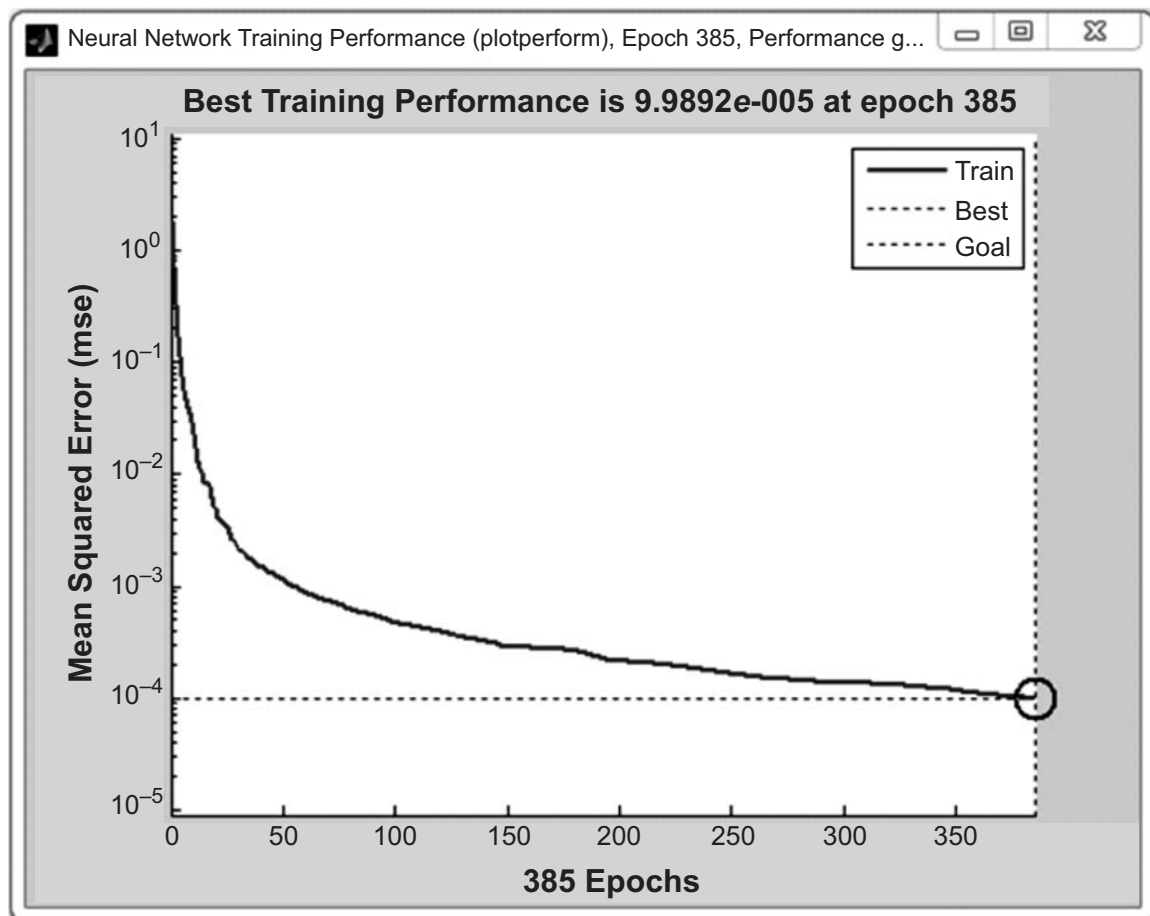


Figure 9: Performance plot of ANN

4. PROPOSED SYSTEM

In this paper, the voltage from the Solar PV array is compared with the reference voltage from the trained artificial neural network to generate the error. This difference in voltage is then given to the PI controller and then compared with a high frequency sine wave to generate duty cycles for the boost converter which then supplies the load. PI controller is used to reduce the steady state error.

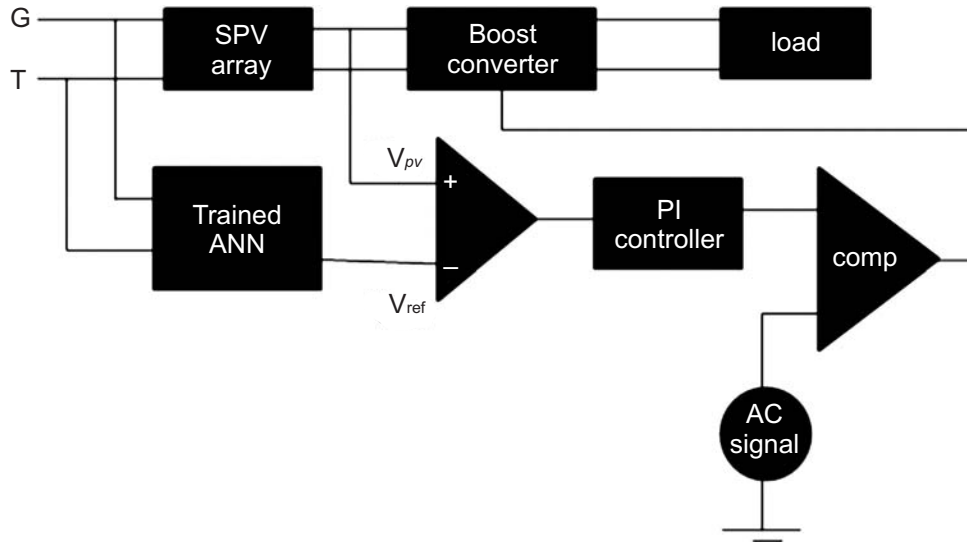


Figure 10: Block diagram of the proposed system

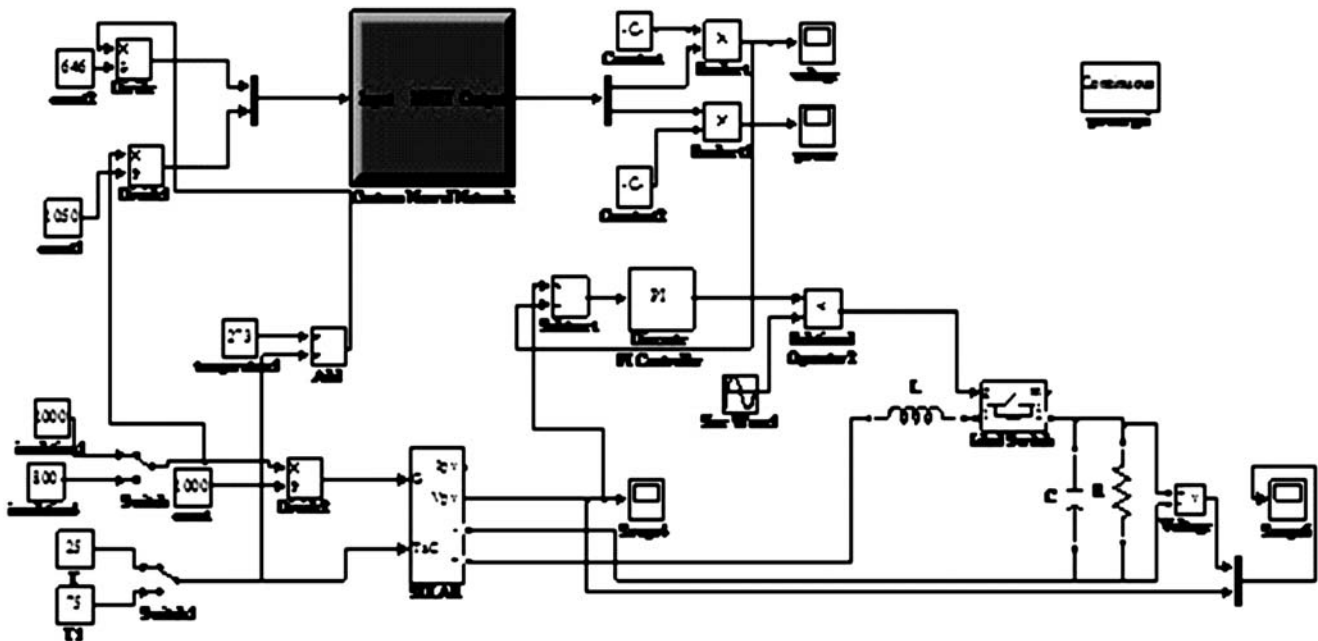


Figure 11: Simulation diagram of the proposed system

5. RESULTS AND DISCUSSION

More number of training data is used for more accurate results. In the Simulation diagram of the proposed system shown in Fig. 11, two manual switches, each for insolation and temperature is used. During simulation of the proposed system, the manual switches are operated in between and the corresponding change in the output voltage is seen in the Fig. 12. The difference in the solar output voltage at the end of PV array and the output voltage obtained using ANN at the end of boost converter is shown in Fig. 12.

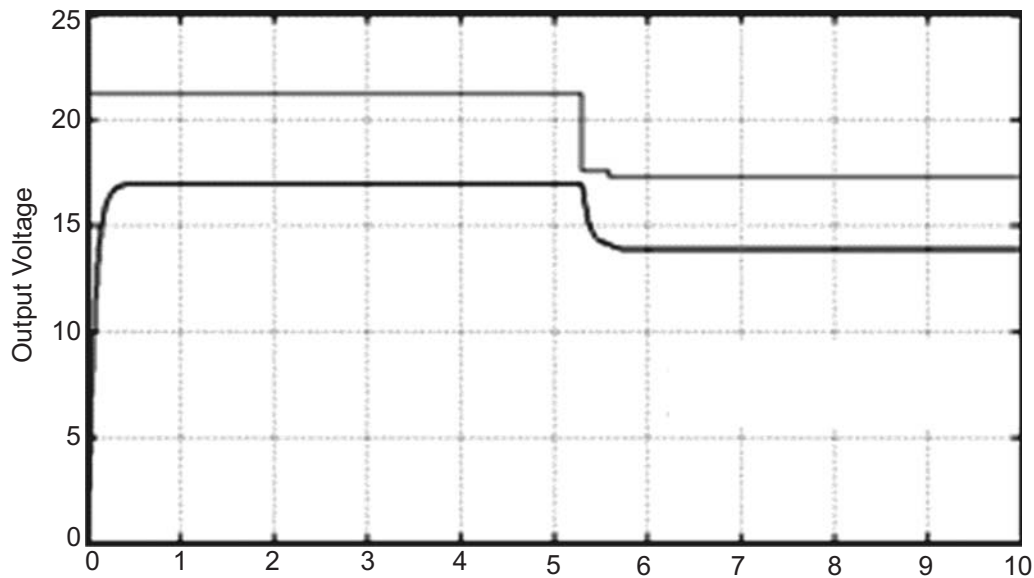


Figure 12: Simulation output voltage

6. CONCLUSION

In this paper modeling of SPV array has been presented. From the modeled SPV array, the voltage corresponding to the maximum power is determined by simulating it for various insolation and temperature. To extract the maximum power from the SPV source, ANN is used. The voltage corresponding to the maximum power for different insolation and temperature has been used for training the ANN. The offline trained ANN is used for providing reference voltage corresponding to maximum power for any environmental changes. The output voltage from the boost converter is similar to that of the reference voltage which gives maximum power.

The result is obtained by training the Neural Network with 1020 data sets. The data variables needed for training the ANN can also be obtained by optimizing values of power using Particle Swarm Optimization (PSO) technique.

7. APPENDIX A DATA FOR TRAINING NEURAL NETWORK

Table 1

<i>Normalised Values</i>			
<i>Temperature</i>	<i>Insolation</i>	<i>Voltage</i>	<i>Power</i>
0.46130031	0.047619048	0.491809246	0.03443159
0.46130031	0.095238095	0.524936294	0.078020465
0.46130031	0.142857143	0.541317801	0.123704455
0.46130031	0.19047619	0.558063342	0.170804768
0.46130031	0.238095238	0.574444849	0.218469395
0.46130031	0.285714286	0.574444849	0.267146926
0.46130031	0.333333333	0.59119039	0.315886398
0.46130031	0.380952381	0.59119039	0.365704605
0.46130031	0.428571429	0.59119039	0.415483053
0.46130031	0.476190476	0.59119039	0.465181983
0.46130031	0.523809524	0.607571897	0.515255246
0.46130031	0.571428571	0.607571897	0.565922692

0.46130031	0.619047619	0.607571897	0.616590139
0.46130031	0.666666667	0.607571897	0.667257586
0.46130031	0.714285714	0.607571897	0.717925033
0.46130031	0.761904762	0.607571897	0.76859248
0.46130031	0.80952381	0.607571897	0.819259927
0.46130031	0.857142857	0.624317437	0.869971197
0.46130031	0.904761905	0.624317437	0.92161524
0.46130031	0.952380952	0.624317437	0.972839412
0.462848297	0.047619048	0.491809246	0.034266212
0.462848297	0.095238095	0.524936294	0.077702734
0.462848297	0.142857143	0.541317801	0.123267594
0.462848297	0.19047619	0.558063342	0.170166736
0.462848297	0.238095238	0.574444849	0.217580837
0.462848297	0.285714286	0.574444849	0.266258368
0.462848297	0.333333333	0.574444849	0.314935899
0.462848297	0.380952381	0.59119039	0.364392553
0.462848297	0.428571429	0.59119039	0.414290278
0.462848297	0.476190476	0.59119039	0.463989208
0.462848297	0.523809524	0.59119039	0.513688138

8. REFERENCES

1. R. J. Wai, W. H. Wang, and C. Y. Lin, "High-performance stand-alone photovoltaic generation system," *IEEE Trans. Ind. Electron.*, vol. 55, no. 1, pp. 240–250, Jan. 2008.
2. J. H. R. Enslin, M. S. Wolf, D. B. Snyman, and W. Sweigers, "Integrated photovoltaic maximum power point tracking converter," *IEEE Trans. Ind. Electron.*, vol. 44, pp. 769–773, Dec. 1997.
3. J. Applebaum, "The quality of load matching in a direct-coupling photovoltaic system," *IEEE Trans. Energy Conversion*, vol. EC-2, pp. 534–541, Dec. 1987.
4. S. M. Alghuwainem, "Matching of a DC motor to a photovoltaic generator using a step-up converter with a current locked loop," *IEEE Trans. Energy Conversion*, vol. 9, pp. 192–198, Mar. 1994.
5. M. M. Saied, A. A. Hanafy, M. A. El-Gabaly, and A. M. Sharaf, "Optimal design parameter for a PV array coupled to a DC motor via a DC–DC transformer," *IEEE Trans. Energy Conversion*, vol. 6, pp. 593–598, Dec. 1991.
6. I. H. Altas and A. M. Sharaf, "A novel on-line MPP search algorithm for PV arrays," *IEEE Trans. Energy Conversion*, vol. 11, pp. 748–754, Dec. 1996.
7. B. K. Bose, P. M. Szczeny, and R. L. Steigerwald, "Microcomputer control of a residential photovoltaic power conditioning system," *IEEE Trans. Ind. Applicat.*, vol. IA-21, pp. 1182–1191, Sept./Oct. 1985.
8. C. Hua, J. Lin, and C. Shen, "Implementation of a DSP-controlled photovoltaic system with peak power tracking," *IEEE Trans. Ind. Electron.*, vol. 45, pp. 99–107, Feb. 1998.
9. K. H. Hussein, I. Muta, T. Hoshino, and M. Osakada, "Maximum photovoltaic power tracking: An algorithm for rapidly changing atmospheric conditions," *Proc. IEE—Generation, Transmission, Distribution*, vol. 142, no. 1, pp. 59–64, Jan. 1995.
10. N. Femia, G. Petrone, G. Spagnuolo, and M. Vitelli, "A technique for improving P&O MPPT performances of double-stage grid-connected photovoltaic systems," *IEEE Trans. Ind. Electron.*, vol. 56, no. 11, pp. 4473–4482, Nov. 2009.
11. R. Alonso, P. Ibáñez, V. Martínez, E. Román, and A. Sanz, "An innovative perturb, observe and check algorithm for partially shaded PV systems," presented at the 13th Eur. Conf. Power Electronics and Applications (EPE'09), Barcelona, Spain, 2009.

12. W. T. Chee, T. C. Green, and A. H.-A. Carlos, "Analysis of perturb and observe maximum power point tracking algorithm for photovoltaic applications," presented at the 2008 IEEE 2nd Int. Power and Energy Conf. (PECon 2008), Johor Bahru, Malaysia, 2008.
13. C. W. Tan, T. C. Green, and C. A. Hernandez-Aramburo, "A current mode controlled maximum power point tracking converter for building integrated photovoltaic's," presented at the 2007 Eur. Conf. Power Electronics and Applications (EPE), Aalborg, Denmark, 2007.
14. A. Pandey, N. Dasgupta, and A. K. Mukerjee, "High-performance algorithms for drift avoidance and fast tracking in solar MPPT system," IEEE Trans. Energy Convers., vol. 23, no. 2, pp. 681–689, Jun. 2008.
15. Al-Atrash, H., Batarseh, I., and Rustom, K. Statistical modeling of DSP based hill-climbing algorithms in noisy environments. In Proceedings of Applied Power Electronics Conference (APEC), 2005, 1773—1777.
16. D. Sera, T. Kerekes, R. Teodorescu, and F. Blaabjerg, Improved MPPT Algorithms for Rapidly Changing Environmental Conditions. Aalborg, Denmark: Aalborg Univ./Inst. Energy Technol., 2006.
17. A. Guechi and M. Chegaar, "Effects of diffuse spectral illumination on microcrystalline solar cells," J. Electron Devices, vol. 5, pp. 116–121, 2007.
18. M. Demirtaş "Design and Implementation of PLC Controlled Solar Tracking System ," e-Journal of new World Sciences Academy, 2009. – No. 4(3) – P. 315–329.
19. T. Hiyama, S. Kouzuma, and T. Imakubo, "Identification of optimal operation point of PV modules using neural network for real time maximum power tracking control," IEEE Trans. Energy Conversion, vol. 10, pp. 360–367, June 1995.
20. T. Hiyama and K. Kitabayashi, "Neural Network Based Estimation of Maximum Power Generation from PV Module Using Environment Information", IEEE Transaction on Energy, Conversion, Vol. 12, NO. 3, pp.241-247, September 1997.